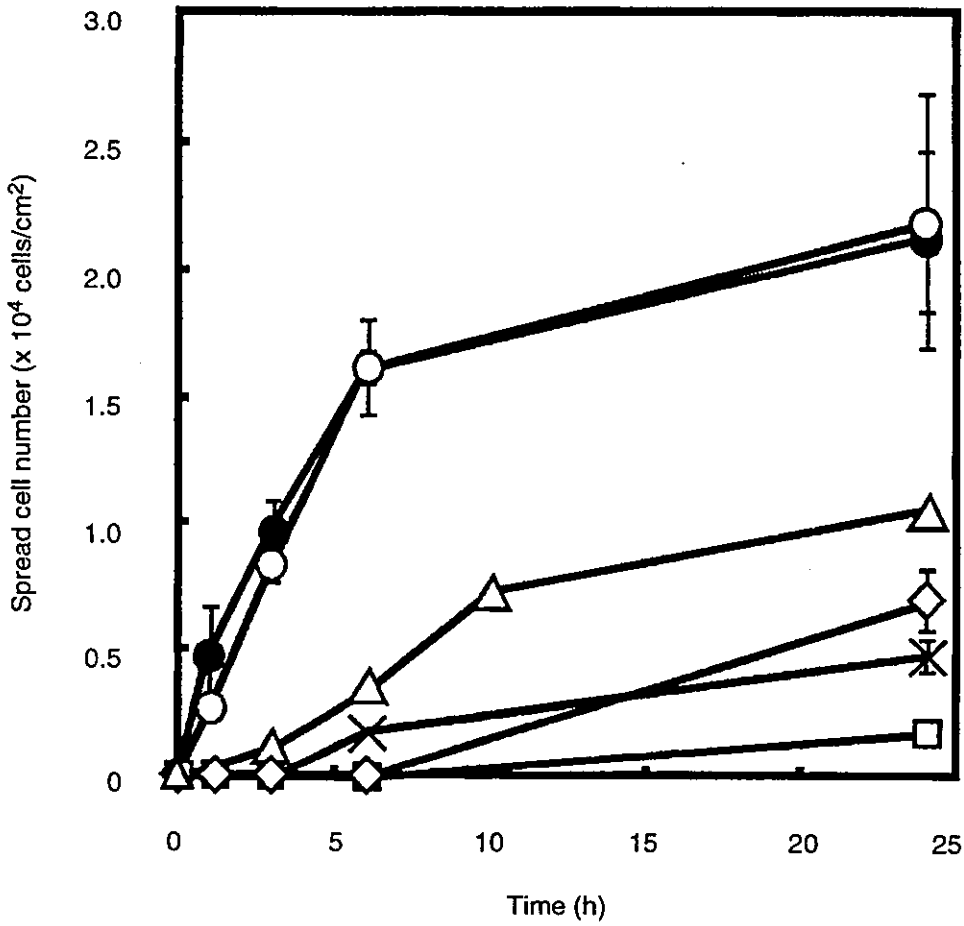

FIG. 5. Competitive assay for BAEC spreading on RGDS-immobilized temperature-responsive surfaces [RGDS(0)-IC(1), mults]). Immobilization of RGDS peptides [RGDS(2)-IC(1), open circles] achieves improvement of BAEC spreading equal to that on 10% FBS supplemented DMEM (solid circles). BAEC spreading on RGDS(2)-IA(1) was suppressed (triangles). BAEC spreading on RGDS(2)-IC(1) was inhibited by preincubation with soluble RGDS peptides (diamonds) and also suppressed at 20°C below the LCST (squares).

immobilization promotes quick cell attachment and growth confluency compared with surfaces before immobilization.

Single-cell and cell sheet detachment by lowering culture temperature

BAECs were challenged to detach from cell-adhesive RGDS-immobilized culture surfaces by reducing the temperature before and after reaching confluency (Figs. 7 and 8). Simply by reducing the culture temperature, single BAECs were spontaneously detached from these surfaces, changing their shapes from spread to round cell morphologies. But the detachment rate was decreased with increasing feed amounts of cell-adhesive peptides (Fig. 7). All spread BAECs were detached from surfaces grafted with less than 5 mol% CIPAAm and 2 mM cell-adhesive peptides. In contrast, few cells detached from the RGDS(2)-IC(10) surface with a high density of immobilized peptides. When the culture temperature was reduced after BAECs reached confluency in growth factor-supplemented serum-free culture, all cells spontaneously detached as a single contiguous cell sheet (Fig. 8), similar to many results we reported previously with pure PIPAAm culture surfaces with serum-containing medium.[1–8]

DISCUSSION

We have previously reported that 5 and 10 mol% feed of CIPAAm comonomer with PIPAAm results in 4.8 and 8.8 mol% incorporation in the linear polymerization in solution.[13] If a similar reaction occurs on the surface, carboxyl groups are introduced onto the temperature-re-

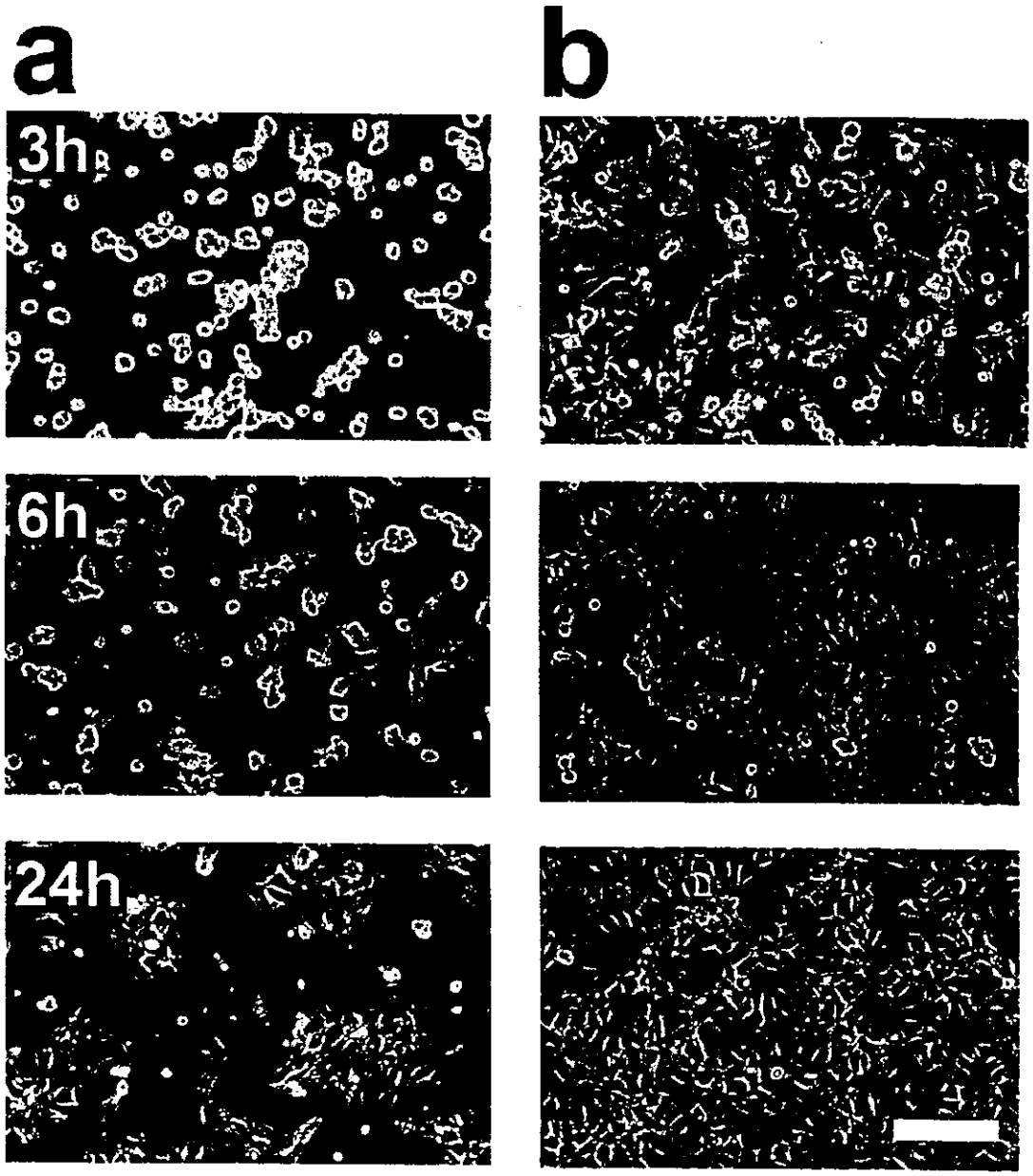

FIG. 6. Phase-contrast photographs of BAEC growth behavior on P(IPAAm-*co*-CIPAAm)-grafted TCPS surfaces before and after RGDS immobilization. Representative cell morphologies after various times in culture with several growth factor supplements at 37°C are shown. (a) IC(1); (b) RGDS(2)-IC(1). Scale bar: 100 μm.

sponsive surface at approximate at densities of 0.2, 0.6, 1.0, and 2.0 nmol/cm^2 for RGDS(X)-IC(1), -IC(3), -IC(5), and -IC(10) surfaces, respectively. These values were calculated on the basis of grafted polymer amounts on surfaces (approximately 2 μg/cm^2) determined by attenuated total reflection Fourier transform infrared (ATR-FTIR) spectra.[14] Actually, cell spreading is increasingly promoted as the carboxyl group density increases on the surface (Fig. 4). However, cell spreading improvement nearly saturates at 1 mol% CIPAAm comonomer in the feed. Feed RGDS concentration also affects BAEC spreading behavior (Fig. 3). Massia and Hubbell reported that the minimal RGD peptide density required for fibroblast spreading was approximately 1 fmol/cm^2.[15] Because cell spreading saturation was observed at a 10^4-fold higher density of carboxyl groups in the present study, only fractional amounts of surface carboxyl groups are reacted and/or only minimal amounts of the surface-immobilized peptides were exposed to cells. Because carbodiimide chemistry was utilized for cell-adhesive peptide immobilization here and the reaction also occurs between the carboxyl terminus of one

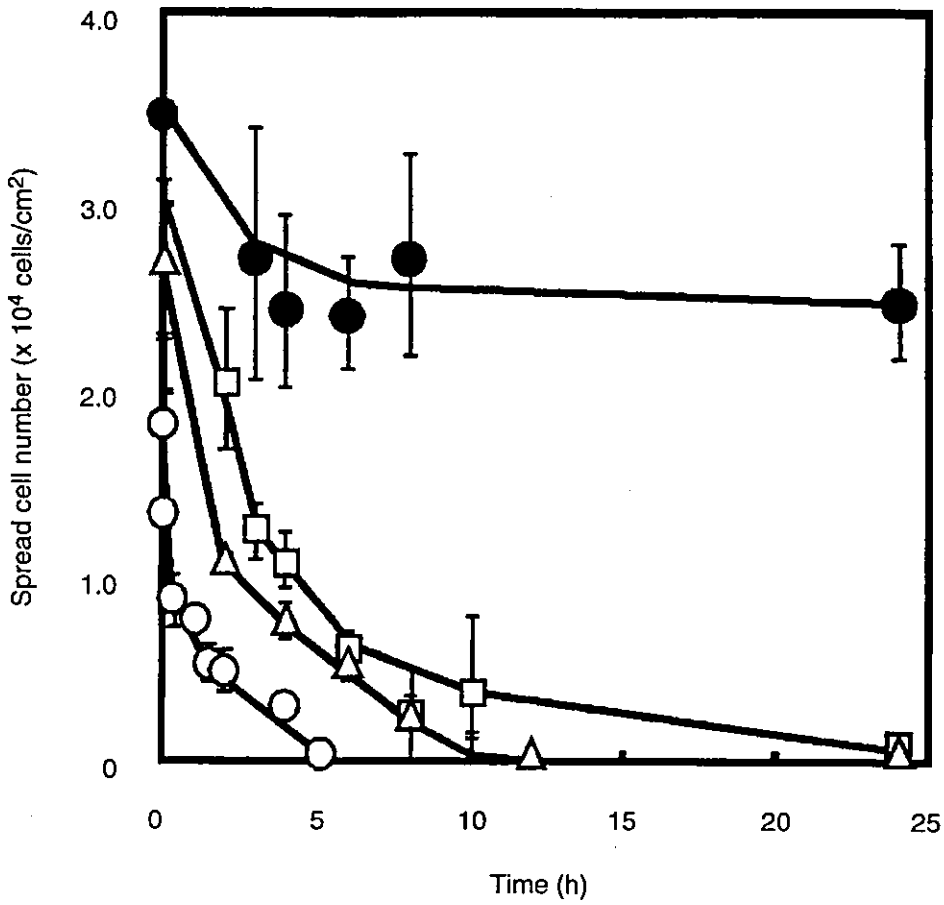

FIG. 7. BAEC detachment from RGDS-immobilized temperature-responsive culture surfaces. RGDS(2)-IC(*X*) surfaces were subjected to low-temperature treatment at 20°C after 24 h of culture at 37°C without serum. CIPAAm compositions: 1 mol% (open circles); 3 mol% (triangles); 5 mol% (squares); and 10 mol% (solid circles).

RGDS peptide and the amino terminus of another RGDS, several synthetic peptides could be linked in tandem. This might explain the higher carboxyl group density required for cell surface saturation. The saturation of feed RGDS concentration for BAEC spreading was observed at 1 mM. This is 50 to 100 times higher than the content of introduced grafted carboxyl groups.

BAEC spreading on RGDS(2)-IA(1) was less than that on RGDS(2)-IC(1) in serum-free culture. Because the intended coupling carboxyl group of acrylic acid (AAc) is closer to its backbone vinyl group than to that of CIPAAm, RGDS peptides are thought to react only with difficulty with the carboxyl groups hindered by neighboring bulky isopropyl groups of IPAAm. Moreover, unreacted carboxyl groups of AAc shift the bulk and surface-grafted copolymer LCST above 37°C whereas those of CIPAAm does not.[13, 14] This LCST shift results in hydration of grafted culture surfaces and hampers cell adhesion at 37°C. Even on RGDS(2)-IC(1), cell seeding below the surface LCST resulted in less cell spreading (Fig. 5). It is plausible that the polymer-grafted surface loses its mechanics and becomes softer below the LCST (Fig. 9). In addition, the density of RGDS exposed to cells decreases under this condition because of the hindrance of hydrated polymer surface chains.

We have previously shown that spread cells detach from PIPAAm-grafted surfaces by lowering the temperature to below the LCST.[1] Because deposited cell-adhesive proteins such as fibronectin and laminin also detach together with cells from the surface of dishes, we concluded that enzyme-free cell detachment from temperature-responsive culture dishes may be attributed to reduced interactions between cell-adhesive proteins and hydrated PIPAAm chains below the LCST.[3,5] In the present study, cell adhesive peptides were covalently immobilized instead of cell-adhesive protein adsorption. Therefore, cell detachment requires dissociation of the immobilized ligands from cell surface integrin receptors.

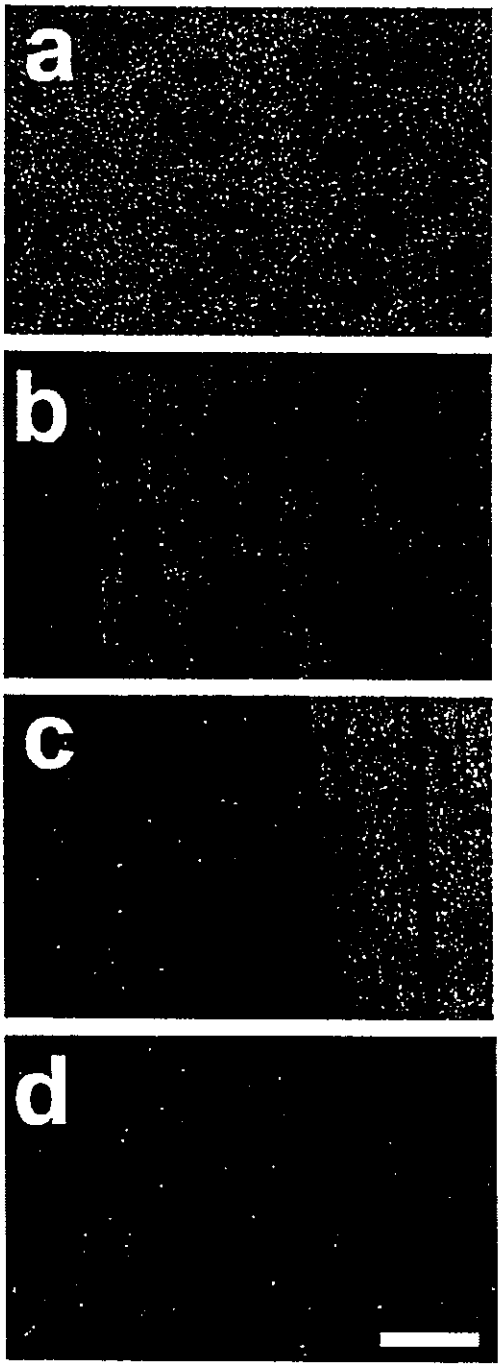

FIG. 8. Harvest of BAEC cultured contiguous sheets from RGDS-immobilized temperature-responsive culture surfaces, RGDS(2)-IC(1), at 20°C below the LCST and under serum-free conditions. (a) 0 min, (b) 60 min, (c) 70 min, and (d) 90 min after reducing culture temperature. Scale bar: 500 μm.

This seems to be a major reason for the retarded cell detachment kinetics compared with that on PIPAAm-grafted surfaces in 10% FBS-supplemented medium.[14] Cell detachment rates in serum-free media decreased with temperature reductions, dependent on immobilized RGDS numbers (Fig. 7). In the case of RGDS-immobilized surfaces containing 10 mol% CIPAAm, RGD(2)-IC(10), 70% of the cultured cells remained spread after 24 h of incubation at 20°C (below the LCST). By contrast, almost all cells detached from RGDS-immobilized surfaces containing less than 5 mol% CIPAAm under these conditions. Interestingly, no significant differences were observed between cells on RGDS(2)-IC(5) and -IC(10) for cell spreading, whereas cell detachment after reducing the temperature was significantly hampered on RGDS(2)-IC(10) in serum-free media. As seen in Figs. 6 and 8, cells would also be recovered as a contiguous monolayer sheet by applying a combination of growth factor supplements.

The main mechanism of cell detachment may involve changes in both polymer-grafted surface rigidity and apparent RGDS density exposed to cells, induced by lowering the temperature. It has been widely reported that cells prefer a stiff substrate to a soft one for their adhesion and downstream cell adhesion events.[16,17] In particular, cells on gradient-compliant hydrogels are likely to move from the soft region toward the stiff region.[18] Mrksich and co-workers also developed a cell detachment system based on an electroactive self-assembled monolayer, and this substrate can selectively detach cells from the surface by releasing ligands.[19] In contrast to their system, our RGDS-immobilized temperature-responsive surface can detach cells from the surface by controlling the binding affinity between ligands and receptors, with RGDS remaining on the cell culture surface.

By introducing synthetic cell-adhesive peptides onto temperature-responsive culture surfaces, both serum-free cell adhesion and noninvasive cell harvest were achieved. Cell proliferation was promoted with growth factors prepared by recombinant technology. By combining the present culture dishes with recombinant growth factors, animal-derived materials can be completely excluded from culture. These techniques would be useful for tissue engineering and other biotechnology applications.

ACKNOWLEDGMENTS

We appreciate the continued useful comments and technical criticisms from Prof. D.W. Grainger (Colorado State University, Fort Collins, CO). This work is supported in part by Grants-in-Aid for Scientific Research by the Ministry of Education, Culture, Sports, Science, and Technology of Japan. The present study is supported in part by the Japanese Ministry for Culture, Sports, Education, Science, and Technology, Core Research for Evolutional Science and Technology (CREST).

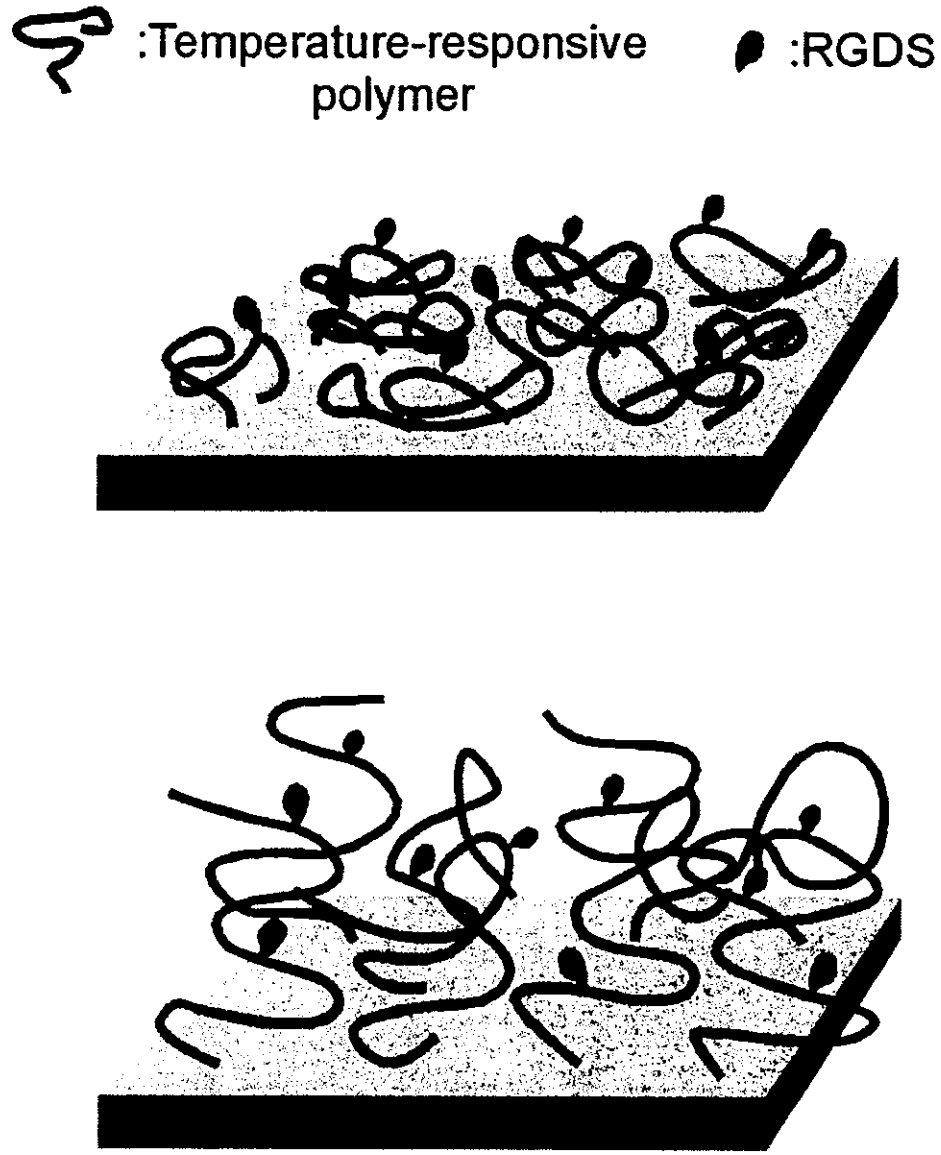

FIG. 9. Schematic illustration of mechanism for serum-free temperature dependence of RGDS-immobilized temperature-responsive surfaces. RGDS peptides were exposed at 37°C (*top*), but were hindered by hydrated polymer chains below the LCST (*bottom*).

REFERENCES

1. Yamada, N., Okano, T., Sakai, H., Karikusa, F., Sawasaki, Y., and Sakurai, Y. Thermoresponsive polymeric surfaces: Control of attachment and detachment of cultured cells. Macromol. Chem. Rapid Commun. **11**, 571, 1990.
2. Yamato, M., Okuhara, M., Karikusa, F., Kikuchi, A., Sakurai, Y., and Okano, T. Signal transduction and cytoskeletal reorganization are required for cell detachment from cell culture surfaces grafted with a temperature-responsive polymer. J. Biomed. Mater. Res. **44**, 44, 1999.
3. Kushida, A., Yamato, M., Konno, C., Kikuchi, A., Sakurai, Y., and Okano, T. Decrease in culture temperature releases monolayer endothelial cell sheets together with deposited fibronectin matrix form temperature-responsive culture surfaces. J. Biomed. Mater. Res. **45**, 355, 1999.
4. Hirose, M., Kwon, O. H., Yamato, M., Kikuchi, A., and Okano, T. Creation of designed shape cell sheets that are noninvasively harvested and moved onto another surface. Biomacromolecules **1**, 377, 2000.
5. Yamato, M., Utsumi, M, Kushida, A., Konno, C., Kikuchi, A., and Okano, T. Thermoresponsive culture dishes allow the intact harvest of multilayered keratinocyte sheets without dispase by reducing temperature. Tissue Eng. **7**, 473, 2001.
6. Kushida, A., Yamato, M., Konno, C., Kikuchi, A., Sakurai, Y., and Okano, T. Temperature-responsive culture dishes allow nonenzymatic harvest of differentiated Madin-

Darby canine kidney (MDCK) cell sheets. J. Biomed. Mater. Res. **51**, 216, 2000.
7. Shimizu, T., Yamato, M., Akutsu, T., Shibata, T., Isoi, Y., Kikuchi, A., Umezu, M., and Okano, T. Electrically communicating three-dimensional cardiac tissue mimic fabricated by layered cultured cardiomyocyte sheet. J. Biomed. Mater. Res. **60**, 110, 2002.
8. Shimizu, T., Yamato, M., Isoi, Y., Akutsu, T., Setomaru, T., Abe, K., Kikuchi, A., Umezu, M., and Okano, T. Fabrication of pulsatile cardiac tissue grafts using a novel 3-dimensional cell sheet manipulation technique and temperature-responsive cell culture surfaces. Circ. Res. **90**, e40, 2002.
9. Erstad, B.L. Implications of prion-induced diseases for animal-derived pharmaceutical products. Am. J. Health System Pharm. **59**, 254, 2002.
10. Wenz, B., Oesch, B., and Horst, M. Analysis of the risk of transmitting bovine spongiform encephalopathy though bone grafts derived from bovine bone. Biomaterials **22**, 1599, 2001.
11. Piershbacher, M.D., and Rouslahti, E. Variants of the cell recognition site of fibronectin that retain attachment-promoting activity. Proc. Natl. Acad. Sci. U.S.A. **81**, 5985, 1984.
12. Hynes, R.O. Integrins: Versatility, modulation, and signaling in cell adhesion. Cell **69**, 11, 1992.
13. Aoyagi, T., Ebara, M., Sakai, K., Sakurai, Y., and Okano, T. Novel bifunctional polymer with reactivity and temperature sensitivity. J. Biomater. Sci. Polym. Ed. **1**, 101, 2000.
14. Ebara, M., Yamato, M., Hirose, M., Aoyagi, T., Sakai, K., and Okano T. Copolymerization of 2-carboxyisopropylacrylamide with *N*-isopropylacrylamide accelerates cell detachment from grafted surfaces by reducing temperature. Biomacromolecules **4**, 344, 2003.
15. Massia, S.P., and Hubbell, J.A. An RGD spacing of 440 nm is sufficient for integrin $\alpha_v\beta_3$-mediated fibroblast spreading and 140 nm for focal contact and stress fiber formation. J. Cell Biol. **114**, 1089, 1991.
16. Wang, H.-B., Dembo, M., and Wang, Y.-L. Substrate flexibility regulates growth and apoptosis of normal but not transformed cells. Am. J. Physiol. Cell. Physiol. **279**, C1345, 2000.
17. Choquet, D., Felsenfeld, D.P., and Sheetz, M.P. Extracellular matrix rigidity causes strengthening of integrin–cytoskeleton linkages. Cell **88**, 39, 1997.
18. Wong, J.Y., Velasco, A., Rajagopalan, P., and Pham, Q. Directed movement of vascular smooth muscle cells on gradient-compliant hydrogels. Langmuir **19**, 1908, 2003.
19. Yeo, W.-S., Hodneland, C.D., and Mrksich, M. Electroactive monolayer substrates that selectively release adherent cells. Chembiochem **7/8**, 590, 2001.

Address reprint requests to:
Teruo Okano, Ph.D.
Institute of Advanced Biomedical Engineering and Science
Tokyo Women's Medical University
8-1 Kawada-cho, Shinjuku-ku
Tokyo 162-8666, Japan

E-mail: tokano@abmes.twmu.ac.jp

ORIGINAL ARTICLE

Corneal Reconstruction with Tissue-Engineered Cell Sheets Composed of Autologous Oral Mucosal Epithelium

Kohji Nishida, M.D., Ph.D., Masayuki Yamato, Ph.D., Yasutaka Hayashida, M.D., Katsuhiko Watanabe, M.Sc., Kazuaki Yamamoto, M.Sc., Eijiro Adachi, M.D., Ph.D., Shigeru Nagai, M.Sc., Akihiko Kikuchi, Ph.D., Naoyuki Maeda, M.D., Ph.D., Hitoshi Watanabe, M.D., Ph.D., Teruo Okano, Ph.D., and Yasuo Tano, M.D., Ph.D.

ABSTRACT

BACKGROUND

Ocular trauma or disease may lead to severe corneal opacification and, consequently, severe loss of vision as a result of complete loss of corneal epithelial stem cells. Transplantation of autologous corneal stem-cell sources is an alternative to allograft transplantation and does not require immunosuppression, but it is not possible in many cases in which bilateral disease produces total corneal stem-cell deficiency in both eyes. We studied the use of autologous oral mucosal epithelial cells as a source of cells for the reconstruction of the corneal surface.

METHODS

We harvested 3-by-3-mm specimens of oral mucosal tissue from four patients with bilateral total corneal stem-cell deficiencies. Tissue-engineered epithelial-cell sheets were fabricated ex vivo by culturing harvested cells for two weeks on temperature-responsive cell-culture surfaces with 3T3 feeder cells that had been treated with mitomycin C. After conjunctival fibrovascular tissue had been surgically removed from the ocular surface, sheets of cultured autologous cells that had been harvested with a simple reduced-temperature treatment were transplanted directly to the denuded corneal surfaces (one eye of each patient) without sutures.

RESULTS

Complete reepithelialization of the corneal surfaces occurred within one week in all four treated eyes. Corneal transparency was restored and postoperative visual acuity improved remarkably in all four eyes. During a mean follow-up period of 14 months, all corneal surfaces remained transparent. There were no complications.

CONCLUSIONS

Sutureless transplantation of carrier-free cell sheets composed of autologous oral mucosal epithelial cells may be used to reconstruct corneal surfaces and can restore vision in patients with bilateral severe disorders of the ocular surface.

From the Department of Ophthalmology, Osaka University Medical School, Osaka (K.N., Y.H., K.W., K.Y., N.M., H.W., Y.T.); the Institute of Advanced Biomedical Engineering and Science, Tokyo Women's Medical University, Tokyo (M.Y., S.N., A.K., T.O.); and the Department of Molecular Morphology, Kitasato University Graduate School of Medicine, Kanagawa (E.A.) — all in Japan. Address reprint requests to Dr. Nishida at the Department of Ophthalmology, Osaka University Medical School, Room E7, Yamadaoka 2-2, Suita, Osaka 565-0871, Japan, or at knishida@ophthal.med.osaka-u.ac.jp.

N Engl J Med 2004;351:1187-96.

CORNEAL EPITHELIAL STEM CELLS RE-side in the basal layer of the limbus,[1,2] the transitional zone between the cornea and the bulbar conjunctiva. These cells govern renewal of the corneal epithelium[3] by generating progeny (transient amplifying cells, which are cells committed to epithelial differentiation) with limited renewal capabilities that migrate from the limbus into the basal layer of the cornea.[4]

If corneal epithelial stem cells are completely absent owing to limbal disorder from severe trauma (e.g., thermal or chemical burns) or eye diseases (e.g., the Stevens–Johnson syndrome or ocular pemphigoid), then the sources of corneal epithelial cells have been exhausted, the peripheral conjunctival epithelium invades inwardly, and the corneal surface becomes enveloped by vascularized conjunctival scar tissue, resulting in corneal opacification that leads to severe visual impairment. Such pathological characteristics are considered to represent limbal stem-cell deficiencies.[5,6]

In patients with unilateral limbal stem-cell deficiency, autologous limbal transplantation is a method of surface reconstruction of the cornea.[7] This procedure, however, requires a large limbal graft from the healthy eye (incurring a risk of causing limbal stem-cell deficiency in the healthy eye[8]), and it is not possible in patients who have bilateral lesions.[9]

Limbal-allograft transplantation can be performed in patients with unilateral or bilateral deficiencies,[10] but it requires long-term immunosuppression that involves high risks of serious eye and systemic complications including infection and liver and kidney dysfunction.[10] In patients with the Stevens–Johnson syndrome or ocular pemphigoid, graft failure is common, even with immunosuppression, owing to serious preoperative conditions such as persistent inflammation of the ocular surface, abnormal epithelial differentiation of the ocular surface, severe dry eye, and lid-related abnormalities.[11-13]

To avoid allograft rejection and improve surgical outcome, some patients with unilateral stem-cell deficiencies have had corneal epithelial grafts constructed ex vivo by the expansion of autologous limbal stem cells harvested from healthy contralateral eyes and cultivated on cell carriers such as amniotic membranes[14,15] and fibrin gel.[16] This process, however, cannot be used for bilateral total limbal stem-cell deficiencies. Therefore, we studied an alternative replacement strategy for damaged corneal epithelium involving a tissue-engineered epithelial-cell sheet comprising only the patient's own oral mucosal epithelial cells. Transplantation of autologous oral mucosal epithelial cells cultured on amniotic membranes to a rabbit corneal model has recently been reported.[17,18]

We studied a new method of transplantation involving a carrier-free cell sheet by exploiting temperature-responsive culture surfaces. By lowering the temperature, we are able to detach all the cultured cells from the surfaces as an intact transplantable cell sheet, and any carrier or scaffold is excluded from the graft.[19] We report the results of ocular-surface reconstruction in four patients with the use of cultured autologous oral mucosal epithelial cells and carrier-free tissue-replacement sheets.

METHODS

SUBJECTS

This study was approved by the institutional review board of Osaka University Medical School, in Osaka, Japan. Oral and written informed consent were obtained from all patients. Patients with bilateral total limbal stem-cell deficiency were eligible for inclusion. Exclusion criteria included glaucoma or xerophthalmia (a skinlike appearance) of the entire ocular surface. Our results are for the first four consecutive patients enrolled, each of whom had one eye grafted with a tissue-engineered epithelial-cell sheet fabricated in culture from harvested autologous oral mucosal epithelial cells in our hospital from January 2003 through March 2003 (Table 1).

All grafted eyes had been clinically diagnosed as having total limbal stem-cell deficiency with complete disappearance of the palisades of Vogt (a radial infolding at the sclerocorneal junction and a biologic marker of the location of corneal epithelial stem cells) and complete coverage by fibrovascular in-growth from 360 degrees of the limbus over the entire cornea. All patients exhibited chronic conjunctival inflammation immunologically driven by the causative diseases reported previously,[20,21] despite therapy with topical steroids. Three of the four patients (Patients 1, 3, and 4) had severe deficiency of the tear film. Lid abnormalities, including chronic blepharitis, misdirection of the eyelashes, and keratinization of the posterior lid margin, contributed to poor ocular-surface conditions and were also noted in all eyes. Patients 1 and 4 had continuous inflammation with severe tear-film and lid abnormalities and keratinization of the ocular

Table 1. Preoperative Characteristics of Patients with Total Limbal Deficiency.

Patient No.	Age	Sex	Diagnosis	Eye	Ocular-Surface Condition			Previous Surgery	Other Eye Diseases
					Symblepharon*	Schirmer's Test without Topical Anesthesia†	Schirmer's Test with Nasal Stimulation‡		
	yr					*mm*			
1	58	M	Stevens–Johnson syndrome (chronic phase)	Right	+	1	2	Allogeneic corneal epithelium (cultivated on amniotic membrane) transplantation in 2000	None
2	69	M	Ocular cicatricial pemphigoid	Left	+	23	26	None	None
3	77	F	Ocular cicatricial pemphigoid	Right	+	1	1	Limbal transplantation with the use of amniotic membrane in 2001	Proliferative diabetic retinopathy, branch-retinal-vein occlusion
4	75	F	Ocular cicatricial pemphigoid	Right	+	1	2	Penetrating keratoplasty in 1999	None

* The plus sign indicates that symblepharon (adhesion of one or both eyelids to the eyeball) was found at the patient's ocular surface.
† Schirmer's test without anesthesia is a commonly used clinical test of lacrimal secretion (tearing). It is performed by measuring the amount of moisture on Whatman filter paper (5 mm by 35 mm) that is placed in the margin of the lower lid for five minutes. A value of less than 5 mm indicates impaired secretion.
‡ Schirmer's test with nasal stimulation is used to measure maximal tearing and is performed by inserting a cotton swab into the nasal cavity. A value of less than 10 mm indicates decreased tearing.

surface. Three of the four patients (Patients 1, 3, and 4) had previously undergone allogeneic grafting, which had failed within one year after surgery, despite systemic and local immunosuppression with cyclosporine (trough levels of 50 to 100 ng per milliliter).

Surgical procedures for all cell-sheet autografts were performed by the same surgeon. A complete ophthalmologic examination included measurement of best corrected visual acuity, slit-lamp biomicroscopy, tonometry, and indirect ophthalmoscopy and was performed in all patients every two to four weeks during the follow-up period, starting two weeks after transplantation. The assessments of visual outcomes were carried out by investigators who were not involved in performing the procedures and were not informed about which eye underwent transplantation or whether the assessment was preoperative or postoperative.

CULTURE AND FABRICATION OF AUTOLOGOUS ORAL MUCOSAL EPITHELIAL-CELL SHEETS

After each patient's oral cavity was sterilized with topical povidone-iodine, a 3-by-3-mm specimen of oral mucosal tissue was surgically excised from the interior buccal mucosal epithelium while the patient was under local anesthesia with xylocaine (Fig. 1A). Oral mucosal epithelial cells were collected by removing all epithelial layers after treatment with dispase II (3 mg per milliliter, Roche), at 37°C for one hour. Collected materials were placed in trypsin and EDTA for 15 minutes to form single-cell suspensions. Temperature-responsive cell-culture inserts (CellSeed) were prepared with the use of commercial cell-culture inserts (Falcon, Becton Dickinson) according to specific procedures described previously.[22] The temperature-responsive polymer poly(*N*-isopropylacrylamide), which reversibly alters its hydration properties with temperature, is chemically immobilized in thin films on cell-culture surfaces, facilitating cell adhesion and growth in normal culture conditions at 37°C. Reducing the temperature of the culture below 30°C causes this surface to hydrate and swell rapidly, prompting complete detachment of adherent cells without the use of typical proteolytic enzymes or treatment with EDTA. Confluent cell cultures on these surfaces can be conveniently harvested as a single, unsupported contiguous cell sheet, retaining cell-to-cell junctions as well as deposited extracellular matrix on the basal surface of the sheet.[23] Enzyme-free harvest permits the cell sheets to be readily manipulated, transferred, layered, or fabricated, because they adhere rapidly to other surfaces, such as traditional culture plastics,[22] other cell sheets, and tissues in vivo.[19]

To prepare lethally treated feeder layers, subconfluent NIH 3T3 cells were incubated with 16 μg of mitomycin C per milliliter for two hours at 37°C and then trypsinized and seeded onto tissue-culture wells (35-mm diameter, Becton Dickinson) at a density of 2×10^4 cells per square centimeter. Oral epithelial cells were separated from these feeder-layer cells during culture with temperature-responsive cell-culture inserts. We confirmed that multilayered cell sheets were fabricated only in the presence of 3T3 cells in the culture system. After culture in vitro for 14 days, epithelial-cell sheets (23.4 mm in diameter) were harvested by reducing the temperature to 20°C.

For colony-forming assays, treatment with trypsin and EDTA was used to isolate single cells from oral mucosal epithelium. Cells were counted, seeded onto culture dishes (35-mm diameter, Becton Dickinson), and cultured with feeder layers treated with mitomycin C. After cultivation for 10 to 12 days, dishes were fixed and stained with rhodamine B. Colony formation in the entire dish was screened under a dissecting microscope.

Figure 1 (facing page). Transplantation of Autologous Tissue-Engineered Epithelial-Cell Sheets Fabricated from Oral Mucosal Epithelium.

Panel A shows the removal of oral mucosal tissue (3 by 3 mm) from patient's cheek. Isolated epithelial cells are seeded onto temperature-responsive cell-culture inserts. After two weeks at 37°C, these cells grow to form multilayered sheets of epithelial cells. The viable cell sheet is harvested with intact cell-to-cell junctions and extracellular matrix in a transplantable form simply by reducing the temperature of the culture to 20°C for 30 minutes. The cell sheet is then transplanted directly to the diseased eye without sutures. In Panel B (the scale bar represents 50 μm), harvested cell sheets have three to five cell layers and do not resemble the original oral mucosa as shown in Panel C (the scale bar represents 100 μm) as closely as they resemble normal corneal epithelium as shown in Panel D (the scale bar represents 100 μm). Panel E shows a transmission electron micrograph of developed microvilli on the apical surface of the cell sheet. Specimens of human tissue-engineered epithelial-cell sheets harvested by reducing the temperature of the culture are immunostained green with anti–keratin 3 antibodies (Panel F), anti–β_1 integrin antibodies (Panel G), and anti-p63 antibodies (Panel H). The nuclei in Panels F, G, and H are shown in red. The scale bars represent 50 μm in Panels F, G, and H. The specimens in Panels B, C, and D are stained with hematoxylin and eosin.

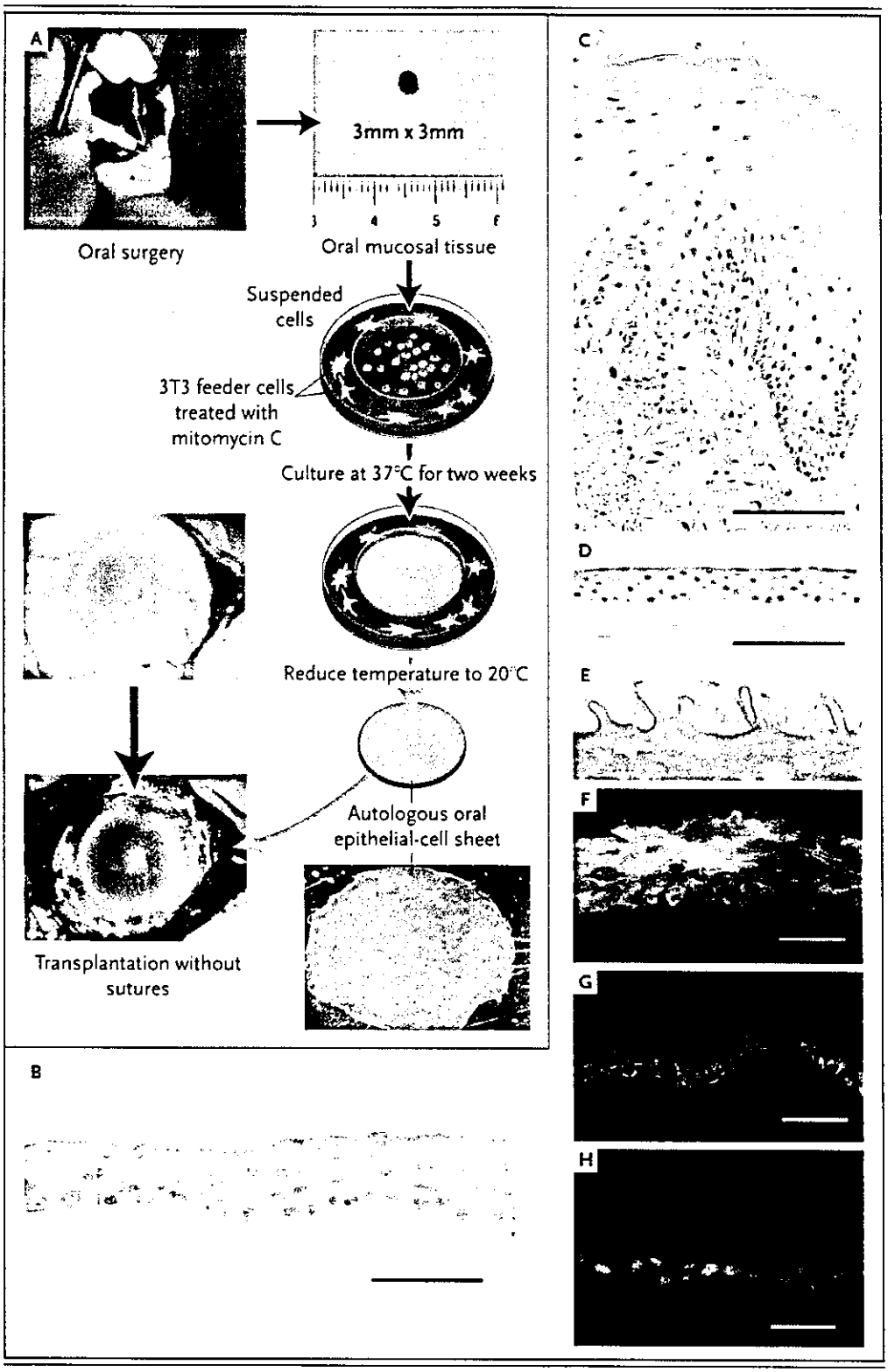
A
Oral surgery
3mm x 3mm
Oral mucosal tissue
Suspended cells
3T3 feeder cells treated with mitomycin C
Culture at 37°C for two weeks
Reduce temperature to 20°C
Autologous oral epithelial-cell sheet
Transplantation without sutures
B
C
D
E
F
G
H

IMMUNOHISTOLOGY

Cryosections from cell sheets were immunostained with monoclonal anti–keratin 3 antibodies (AE5, Progen Biotechnik), anti–β_1 integrin antibodies (P5D2, Santa Cruz Biotechnology), or anti-p63 antibodies (4A4, Santa Cruz Biotechnology) and fluorescein isothiocyanate–labeled or rhodamine-labeled secondary antibodies (Jackson ImmunoResearch Laboratories). Nuclei were costained with Hoechst 33342 (Molecular Probes) or propidium iodide (Sigma). Stained cells were observed using confocal laser scanning microscopy (LSM-510, Zeiss). The same concentration of corresponding normal nonspecific IgG provided negative controls, and native human corneal and limbal tissues were used as positive controls.

TRANSPLANTATION OF CELL SHEETS TO THE EYE

We removed the conjunctival and subconjunctival scar tissue from the cornea up to 3 mm outside the limbus to reexpose corneal stroma (Fig. 2, and a video clip in the Supplementary Appendix, available with the full text of this article at www.nejm.org). Subsequently, the harvested sheet of autologous oral mucosal epithelial cells was placed directly onto the exposed transparent stromal bed as described previously.[6,23] No sutures were required. The grafted corneal surface was then covered with a soft contact lens for protection during healing. After surgery, topical antibiotics (0.3 percent ofloxacin) and steroids (0.1 percent betamethasone) were initially applied four times a day and then tapered to three times a day. During the first week after surgery, betamethasone (1 mg per day) was administered orally to reduce postoperative inflammation. One month after surgery, the administration of topical corticosteroids was changed from 0.1 percent betamethasone to 0.1 percent fluorometholone. Because the patients had severe dry eye, proper wound healing could not be expected without tear supplementation. Preservative-free artificial tears were frequently used, and the puncta lacrimale of all the patients were occluded to increase tear retention.

RESULTS

CHARACTERIZATION OF TISSUE-ENGINEERED EPITHELIAL-CELL SHEETS

We compared cultured autologous oral mucosal-cell sheets with endogenous tissue both functionally and phenotypically. Oral mucosal epithelial cells cultured under these culture conditions resemble corneal epithelium, with three to five cell layers, small basal cells, flattened middle cells, and polygonal and flattened superficial cells (Fig. 1B), more than they resemble native oral mucosal epithelium (Fig. 1C), which is much thicker than corneal epithelium (Fig. 1D). The optical transparency of harvested cell sheets was equal to that of corneal epithelial-cell sheets originating from limbal stem cells (data not shown).[23]

Ultrastructural examination revealed an architecture of well-structured, compact, multilayered cell sheets with the expected microstructures of the native cells, including microvilli (Fig. 1E), tight junctions, desmosomes, and basement membrane. Such morphologic characteristics are similar to those of corneal epithelium in vivo. Native corneal epithelial cells and oral mucosal epithelial cells express keratin 3 as a characteristic phenotypic marker, and harvested epithelial-cell sheets also express keratin 3 (Fig. 1F).

The mean (±SE) colony-forming efficiency, calculated as the ratio of the number of stem or progenitor cells that can produce colonies to the total number of cells in the harvested tissue, was 2.1±0.9 percent for all four patients (with measurements performed in triplicate in each patient), confirming the presence of progenitor cells among the isolated oral mucosal epithelial cells. Correspondingly, β_1 integrin, reported to be an epithelial stem-cell and progenitor-cell marker[24] susceptible to digestion by trypsin, remained intact in the basal cells (Fig. 1G). The basal cells in the multilayered cell sheets also express p63 (Fig. 1H), a putative epithelial stem-cell marker.[25]

CLINICAL RESULTS OF TRANSPLANTATION OF THE CELL SHEET TO THE CORNEAL SURFACE

Attachment of the cell sheet to the stromal bed was spontaneous and uniform (Fig. 2, and video clip in the Supplementary Appendix). Within several minutes after placement without sutures, the grafted cell sheets remained intact and stably bound to the stromal surfaces, even after the extensive application of eyedrops. This observation is consistent with previous experiments with rabbit models, in which transplanted sheets of oral mucosal epithelial cells readily resisted outward displacement when the perimeters were pulled with forceps.

Immediately after surgery, the transplanted corneal surface was clear and smooth, without observable vascularization. Within one week, slit-lamp ex-

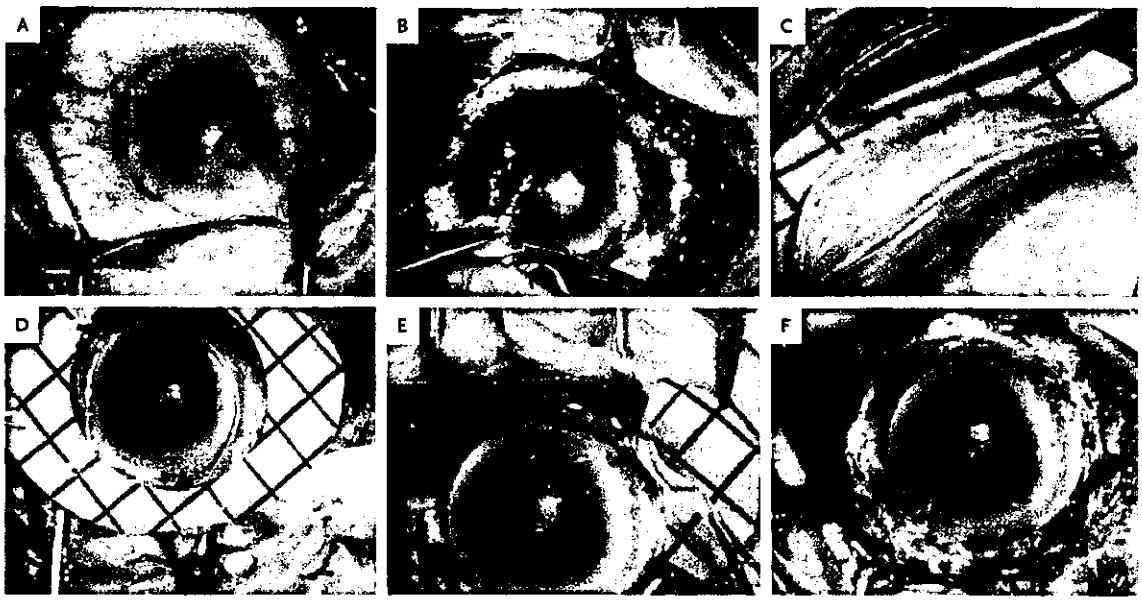

Figure 2. Transplantation Procedures for Tissue-Engineered Autologous Epithelial-Cell Sheets.

Preoperatively, the entire corneal surface was covered by conjunctival tissue with neovascularization (Panel A). In Panel B, conjunctival tissue over the cornea is surgically removed to reexpose transparent corneal stroma. Then, the sheet of tissue-engineered epithelial cells is harvested from a temperature-responsive culture insert with the use of a doughnut-shaped supporter ([black-and-white squares] Panel C) and placed on the stromal bed (Panel D). The sheet adheres to corneal stroma in a few minutes without sutures, and the supporter is removed (Panel E), leaving the cell sheet on the stroma (Panel F). A video clip can be viewed in the Supplementary Appendix, available with the full text of this article at www.nejm.org.

amination with fluorescein sodium staining showed complete reepithelialization of the corneal surface in all four eyes, revealing the tight junction-mediated barrier function. Corneal transparency was restored without any defects of the corneal epithelium. In all eyes, stromal vascularization gradually recurred in the peripheral cornea but not in the central zone. This vascularization was unlike subepithelial vascularization accompanied by conjunctival ingrowth, since it was localized to the deeper stroma and did not show the abnormally high fluorescein permeability characteristic of conjunctival epithelium.

During a mean follow-up period of 14 months, corneal transparency was maintained (Fig. 3 and Table 2). Maximally improved visual acuity was obtained 6, 2, 10, and 8 weeks after transplantation for Patients 1 through 4, respectively, and became stable thereafter. The length of time until visual acuity improved seemed to correspond to the length of time until the corneal stroma became less opaque. No complications were observed.

DISCUSSION

Our study shows that tissue-engineered cell sheets from autologous oral mucosal epithelium may serve as effective substitutes for allografts of limbal tissue in the reconstruction of the corneal and limbal surfaces. Four patients (four eyes) were consecutively treated with this approach, and corneal transparency was restored and postoperative visual acuity improved remarkably (Table 2). During the follow-up period, all corneal surfaces remained transparent, and there were no serious complications.

We developed this strategy on the basis of several observations from cell biology and medicine. First, in vivo oral mucosal epithelium expresses keratin 3, which is also expressed by the corneal epithelium but not by the epidermis.[1,27] Second, the excision of a small piece of oral mucosal tissue from the patient is straightforward, and the resulting wound heals within several days without incident or scarring. Third, transplantation of autologous

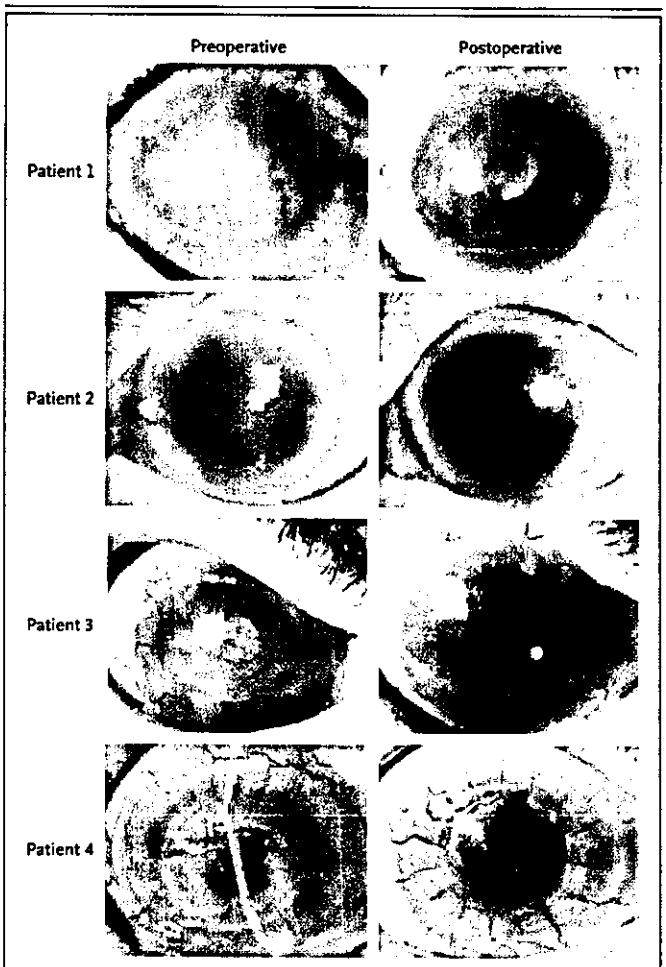

Figure 3. Eyes of Patients before and after Transplantation of Sheets of Tissue-Engineered Autologous Epithelial Cells.

These photographs were taken just before transplantation of the cell sheets and postoperatively at 13, 14, or 15 months.

buccal mucosal grafts directly onto ocular surfaces was previously reported in human patients[28] for the purposes of treating corneal ulcers, corneal perforations, and lid abnormalities (e.g., marginal entropion and trichiasis); these grafts are not useful for improving vision, since they contain opaque subepithelial fibrous tissue. In contrast, the transparency of carrier-free sheets of tissue-engineered epithelial cells fabricated from oral mucosal epithelial cells is similar to the transparency of corneal epithelial-cell sheets originating from limbal stem cells.[23]

Reconstruction with autologous oral mucosal epithelial cells offers substantial clinical advantages over allogeneic transplantation for treating severe diseases such as the Stevens–Johnson syndrome and ocular pemphigoid. It averts the risks of allogeneic immunorejection and immunosuppression. Severe tear-film and lid abnormalities often associated with these diseases continue to be a challenge, since immunologically driven inflammation of the ocular surface persists chronically in these patients.

Although decisive epithelial stem-cell markers that could provide evidence of the presence of these stem cells in grafted cell sheets have not yet been established,[29] results from colony-forming assays for oral mucosal epithelium show that excised oral tissue contains epithelial stem cells or at least progenitor cells. Since ocular surfaces that have been grafted with cell sheets retain their transparency for more than one year, and because the life spans of transient amplifying cells (cells committed to epithelial differentiation) are believed to be less than one year,[30] we conclude that progenitor cells with the potential to differentiate into new corneal epithelial phenotype are present in autografts of cell sheets.

Conjunctival epithelial cells invade the cornea after allogeneic transplantation because of the gradual depletion of allogeneic corneal epithelial cells due to epithelial rejection or stem-cell depletion.[31-33] It is unknown whether this also applies to autologous transplants. In the four eyes we studied, limited stromal vascularization occurred within a few months after transplantation of the cell sheet and reached a stable state within six months, with no appreciable growth thereafter. This stromal vascularization was observed only beneath cell sheets on peripheral corneas and should be distinguished from the subepithelial neovascularization accompanied by conjunctival ingrowth that results from the stem-cell loss associated with allografts, which occurs several months after transplantation. This finding suggests that grafted oral mucosal epithelial cells remained on the ocular surface.

It is possible that the reduction in host immunologic reactions associated with the grafting of autologous cells may minimize epithelial rejection, but further study is needed. The limited stromal neovascularization that we observed is probably caused by angiogenic factors secreted from tissue-engineered epithelial-cell sheets fabricated from oral mucosal epithelial cells originally located in

Table 2. Surgical Outcome in Four Patients Who Received Transplants of Tissue-Engineered Autologous Oral Mucosal-Cell Sheets.

Patient No.	Best Corrected Visual Acuity in Damaged Eye		Corneal Opacity (Grade)*			Complication	Months of Follow-up
	Preoperative†	Postoperative	Preoperative	1 Month after Surgery	At Last Observation		
1	Counting fingers	20/100	3	2	1	None	15
2	20/2000	20/25	3	1	1	None	14
3	Hand motion	20/300	3	1	1	None	14
4	20/2000	20/50	3	1	1	None	13

* The extent of corneal opacity was graded by three masked observers on the basis of the slit-lamp examination with a previously described system[26] and modifications for ocular-surface diseases. Grade 0 indicates clear or trace haze, grade 1 mild opacity, grade 2 moderately dense opacity partially obscuring details of the iris, and grade 3 severely dense opacity obscuring details of the intraocular structure. Grading is based on the opacity observed in all corneal layers, including epithelium, stroma, and endothelium.

† The visual acuity of patients who could not read a visual-acuity chart at a distance of 0.5 m was assessed by asking whether they could see the number of fingers held up by the examiner. If they could not, visual acuity was assessed by the patient's ability to see hand movement by the examiner.

vivo on the substantia propria, which is rich in vessels. However, the production of antiangiogenic factors such as thrombospondin by keratocytes[34] may limit vascularization to peripheral areas.

We observed that the transplanted cell sheets became more transparent and achieved smoother, integrated surfaces on the corneal stroma, further resembling normal corneal epithelium; a plateau was reached one to three months after transplantation. Originally, oral mucosal epithelium, located on substantia propria, is morphologically distinct from corneal epithelium in that it is much thicker and multilayered and has an irregular surface (Fig. 1C). The use of temperature-responsive harvesting allows the grafted carrier-free oral mucosal epithelial cells to interact immediately and directly with patients' corneal stromal keratocytes without interference from cell carriers such as fibrin gel and amniotic membranes.

Our transplantable epithelial-cell sheets used the common 3T3 feeder-layer method originally developed for the production of autologous epidermal-cell grafts[35] and used in the culture of other epithelial cells from various tissue sources, including the limbus.[16] This method has been clinically applied since the 1980s for the treatment of various skin conditions, including burns and giant nevi, although the Food and Drug Administration classifies these grafts as xenografts.

In summary, we have shown that sheets of tissue-engineered epithelial cells fabricated ex vivo from autologous oral mucosal epithelium are effective for reconstructing the ocular surface and restoring vision in patients with bilateral total stem-cell deficiencies. Long-term follow-up and experience with a large series of patients are needed to assess further the benefits and risks of this method, which offers the potential to treat severe ocular diseases that are resistant to standard approaches.

Supported by Grants-in-Aid for Scientific Research (15390530, 16200036, and 16300161), the High-Tech Research Center Program, and the Center of Excellence Program for the 21st Century from the Ministry of Education, Culture, Sports, Science, and Technology in Japan and by the Core Research for Evolution Science and Technology from the Japan Science and Technology Agency.

We are indebted to Professor David Grainger, Colorado State University, and Mr. Joseph Yang, Tokyo Women's Medical University, for their technical review.

REFERENCES

1. Schermer A, Galvin S, Sun TT. Differentiation-related expression of a major 64K corneal keratin in vivo and in culture suggests limbal location of corneal epithelial stem cells. J Cell Biol 1986;103:49-62.
2. Cotsarelis G, Cheng SZ, Dong G, Sun TT, Lavker RM. Existence of slow-cycling limbal epithelial basal cells that can be preferentially stimulated to proliferate: implications on epithelial stem cells. Cell 1989;57:201-9.
3. Thoft RA, Friend J. The X, Y, Z hypothesis of corneal epithelial maintenance. Invest Ophthalmol Vis Sci 1983;24:1442-3.
4. Buck RC. Measurement of centripetal migration of normal corneal epithelial cells in the mouse. Invest Ophthalmol Vis Sci 1985; 26:1296-9.
5. Tseng SC. Concept and application of limbal stem cells. Eye 1989;3:141-57.
6. Nishida K. Tissue engineering of the cornea. Cornea 2003;22:Suppl 7:S28-S34.

7. Kenyon KR, Tseng SC. Limbal autograft transplantation for ocular surface disorders. Ophthalmology 1989;96:709-22.
8. Chen JJ, Tseng SC. Corneal epithelial wound healing in partial limbal deficiency. Invest Ophthalmol Vis Sci 1990;31:1301-14.
9. Dua HS, Azuara-Blanco A. Autologous limbal transplantation in patients with unilateral corneal stem cell deficiency. Br J Ophthalmol 2000;84:273-8.
10. Tsubota K, Satake Y, Kaido M, et al. Treatment of severe ocular-surface disorders with corneal epithelial stem-cell transplantation. N Engl J Med 1999;340:1697-703.
11. Samson CM, Nduaguba C, Baltatzis S, Foster CS. Limbal stem cell transplantation in chronic inflammatory eye disease. Ophthalmology 2002;109:862-8.
12. Ilari L, Daya SM. Long-term outcomes of keratolimbal allograft for the treatment of severe ocular surface disorders. Ophthalmology 2002;109:1278-84.
13. Shimazaki J, Shimmura S, Fujishima H, Tsubota K. Association of preoperative tear function with surgical outcome in severe Stevens-Johnson syndrome. Ophthalmology 2000;107:1518-23.
14. Schwab IR, Reyes M, Isseroff RR. Successful transplantation of bioengineered tissue replacements in patients with ocular surface disease. Cornea 2000;19:421-6.
15. Tsai RJ, Li LM, Chen JK. Reconstruction of damaged corneas by transplantation of autologous limbal epithelial cells. N Engl J Med 2000;343:86-93.
16. Rama P, Bonini S, Lambiase A, et al. Autologous fibrin-cultured limbal stem cells permanently restore the corneal surface of patients with total limbal stem cell deficiency. Transplantation 2001;72:1478-85.
17. Nakamura T, Endo K, Cooper LJ, et al. The successful culture and autologous transplantation of rabbit oral mucosal epithelial cells on amniotic membrane. Invest Ophthalmol Vis Sci 2003;44:106-16.
18. Kinoshita S, Nakamura T. Development of cultivated mucosal epithelial sheet transplantation for ocular surface reconstruction. Artif Organs 2004;28:22-7.
19. Yamato M, Okano T. Cell sheet engineering. Mater Today 2004;May:42-7.
20. Kawasaki S, Nishida K, Sotozono C, Quantock AJ, Kinoshita S. Conjunctival inflammation in the chronic phase of Stevens-Johnson syndrome. Br J Ophthalmol 2000;84:1191-3.
21. Foster CS, Fong LP, Azar D, Kenyon KR. Episodic conjunctival inflammation after Stevens-Johnson syndrome. Ophthalmology 1988;95:453-62.
22. Hirose M, Kwon OH, Yamato M, Kikuchi A, Okano T. Creation of designed shape cell sheets that are noninvasively harvested and moved onto another surface. Biomacromolecules 2000;1:377-81.
23. Nishida K, Yamato M, Hayashida Y, et al. Functional bioengineered corneal epithelial sheet grafts from corneal stem cells expanded ex vivo on a temperature-responsive cell culture surface. Transplantation 2004;77:379-85.
24. Jones PH, Watt FM. Separation of human epidermal stem cells from transit amplifying cells on the basis of differences in integrin function and expression. Cell 1993;73:713-24.
25. Pellegrini G, Dellambra E, Golisano O, et al. p63 Identifies keratinocyte stem cells. Proc Natl Acad Sci U S A 2001;98:3156-61.
26. Fantes FE, Hanna K, Waring GO III, Pouliquen Y, Thompson KP, Salvodelli M. Wound healing after excimer laser keratomileusis (photorefractive keratectomy) in monkeys. Arch Ophthalmol 1990;108:665-75.
27. Moll R, Franke WW, Schiller DL, Geiger B, Krepler R. The catalog of human cytokeratins: patterns of expression in normal epithelia, tumors and cultured cells. Cell 1982;31:11-24.
28. Shore JW, Foster CS, Westfall CT, Rubin PA. Results of buccal mucosal grafting for patients with medically controlled ocular cicatricial pemphigoid. Ophthalmology 1992;99:383-95.
29. Dua HS, Joseph A, Shanmuganathan VA, Jones RE. Stem cell differentiation and the effects of deficiency. Eye 2003;17:877-85.
30. Kinoshita S, Friend J, Thoft RA. Sex chromatin of donor corneal epithelium in rabbits. Invest Ophthalmol Vis Sci 1981;21:434-41.
31. Holland EJ, Schwartz GS. Epithelial stem-cell transplantation for severe ocular-surface disease. N Engl J Med 1999;340:1752-3.
32. Shimazaki J, Kaido M, Shinozaki N, et al. Evidence of long-term survival of donor-derived cells after limbal allograft transplantation. Invest Ophthalmol Vis Sci 1999;40:1664-8.
33. Williams KA, Brereton HM, Aggarwal R, et al. Use of DNA polymorphisms and the polymerase chain reaction to examine the survival of a human limbal stem cell allograft. Am J Ophthalmol 1995;120:342-50.
34. Hiscott P, Sorokin L, Nagy ZZ, Schlotzer-Schrehardt U, Naumann GO. Keratocytes produce thrombospondin 1: evidence for cell phenotype-associated synthesis. Exp Cell Res 1996;226:140-6.
35. Rheinwald JG, Green H. Serial cultivation of strains of human epidermal keratinocytes: the formation of keratinizing colonies from single cells. Cell 1975;6:331-43.

POSTING PRESENTATIONS AT MEDICAL MEETINGS ON THE INTERNET

Posting an audio recording of an oral presentation at a medical meeting on the Internet, with selected slides from the presentation, will not be considered prior publication. This will allow students and physicians who are unable to attend the meeting to hear the presentation and view the slides. If there are any questions about this policy, authors should feel free to call the *Journal*'s Editorial Offices.

Available online at www.sciencedirect.com
SCIENCE DIRECT®
Surface Science 570 (2004) 134–141
SURFACE SCIENCE
www.elsevier.com/locate/susc

Incorporation of new carboxylate functionalized co-monomers to temperature-responsive polymer-grafted cell culture surfaces

Mitsuhiro Ebara [a], Masayuki Yamato [b], Shigeru Nagai [b], Takao Aoyagi [b], Akihiko Kikuchi [b], Kiyotaka Sakai [a], Teruo Okano [b,*]

[a] *Department of Applied Chemistry, Waseda University, 3-4-1 Ohkubo, Shinjuku-ku, Tokyo 169-8555, Japan*
[b] *Institute of Advanced Biomedical Engineering and Science, Tokyo Women's Medical University, 8-1 Kawada-cho, Shinjuku-ku, Tokyo 162-8666, Japan*

Available online 10 July 2004

Abstract

Several cultured cell types are easily detached from poly(*N*-isopropylacrylamide) (PIPAAm)-grafted surfaces only by reducing culture temperature without traditional proteolytic treatments that might damage certain cell functions. We have exploited these novel surfaces for tissue engineering applications where harvested intact cell sheets are useful for fabricating tissue-like constructs. We now extend the polymer chemistry of such grafted surfaces with new charged co-monomers. Functional carboxylate groups are incorporated into temperature-responsive surfaces with newly designed analogous carboxylate co-monomers, 2-carboxyisopropylacrylamide (CIPAAm) and 3-carboxy-*n*-propylacrylamide (CNPAAm), which have a small structural difference in the placement of the carboxylate group (*iso* or *normal* to the monomer propyl group). P(IPAAm-*co*-CIPAAm) demonstrates a similar phase transition behavior to that of pure PIPAAm, and the ionic dissociation of carboxyl groups is suppressed (elevated p*K*'a) even under physiological conditions. By contrast, P(IPAAm-*co*-CNPAAm) exhibits a higher charge density (lower p*K*'a), higher hydration, and reduced temperature-sensitivity under identical conditions. Introduction of 5 mol% CNPAAm into PIPAAm grafted surfaces produces no cell attachment under typical cell culture conditions, while identical introductions of CIPAAm into grafted copolymers functions well for cell attachment. Cultured cell spreading efficiency was essentially similar on PIPAAm-grafted surfaces as on copolymer-grafted surfaces with 1 mol% introduction of either carboxylate co-monomer. Accelerated cell detachment upon reducing culture temperature was observed for the 1 mol% these copolymer-grafted surfaces since polymer hydration and swelling kinetics are enhanced by the increased ionizable moiety in these grafted surfaces.

* Corresponding author. Tel.: +81 3 3353 8111x30233; fax: +81 3 3359 6046.
E-mail address: tokano@abmes.twmu.ac.jp (T. Okano).

0039-6028/$ - see front matter © 2004 Elsevier B.V. All rights reserved.
doi:10.1016/j.susc.2004.06.183

Keywords: Carboxylic acid; Surface structure, morphology, roughness, and topography

1. Introduction

Poly(*N*-isopropylacrylamide) (PIPAAm) is a water-soluble polymer below its lower critical solution temperature (LCST) of 32 °C [1,2]. This polymer becomes hydrophobic and undergoes reversible phase separation as temperature increases above the LCST. Over the past decade, a considerable number of studies have demonstrated new biomedical applications for PIPAAm, such as intelligent surfaces for bioseparation systems [3,4] and enzyme-free cell culture/harvest systems [5–7]. We have succeeded in surface interaction control with bioactive molecules and cultured cells by exploiting the reversible, temperature-sensitive properties of PIPAAm-grafted surfaces [3–10]. Functionalization of PIPAAm has also been attempted by co-polymerization of IPAAm with other functional co-monomers such as acrylic acid (AAc) [11–13]. However, introduction of other co-monomers often results in reduced temperature sensitivity [14–16]. Particularly, IPAAm copolymers with AAc exhibit a dramatically decreased magnitude of the polymer temperature-sensitive phase transition under physiological conditions (pH 7.4), rendering them impractical for many applications.

In order to overcome these shortcomings, we have designed new functionalized monomers based on the hypothesis that the sharp phase transition behavior observed for PIPAAm results from the alignment of side chain isopropyl groups upon dehydration. We have therefore synthesized 2-carboxyisopropylacrylamide (CIPAAm) having a similar side chain structure of IPAAm [16,17]. IPAAm co-polymers with CIPAAm show sensitive phase transition in response to temperature change, and the LCST is almost the same as that of the IPAAm homopolymer. We have now newly synthesized the analogous monomer, 3-carboxyl-*n*-propylacrylamide (CNPAAm). The only difference from CIPAAm is the propyl side group: *iso*-versus *normal* (see Fig. 1), producing a distinct structural difference in the alignment of the side chain propyl group under hydration, and allowing us to test the hypothesis that this will affect the polymer phase transition. The phase transition behavior and temperature-responsive cell attachment/detachment on these copolymer-grafted surfaces were examined and compared. Distinct differences are observed, allowing us to conclude that the side chain functional group position is important to retain thermally sensitive properties while providing functional co-monomer chemistry.

2. Materials and methods

2.1. Monomer preparation

N-Isopropylacrylamide (IPAAm) was kindly provided from Kojin Co. (Tokyo, Japan) and puri-

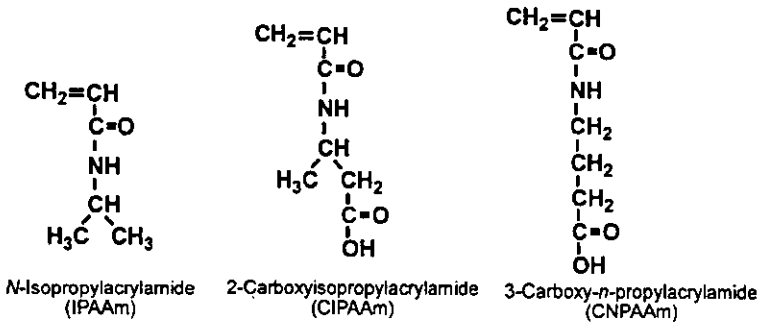

Fig. 1. Chemical structures for *N*-isopropylacrylamide (IPAAm), 2-carboxyisopropylacrylamide (CIPAAm), and 3-carboxy-*n*-propylacrylamide (CNPAAm) monomers.

fied by recrystallization from *n*-hexane. CIPAAm monomer was synthesized as described previously [16]. Briefly, D,L-3-aminobutyric acid (purity 98%, Tokyo Kasei, Tokyo, Japan) was esterified using benzyl alcohol. Acryloyl chloride was reacted with the benzyl ester in the presence of triethylamine. CIPAAm was obtained by hydrolysis of the benzyl ester using sodium hydroxide aqueous solution. Protonation of carboxyl groups was carried out using an excess amount of hydrochloric acid. CNPAAm monomer was similarly synthesized but using D,L-4-aminobutyric acid in place of D,L-3-aminobutyric acid. Both monomers were certified by NMR and were stored as viscous oil at 4 °C under nitrogen prior to polymerization.

2.2. Synthesis of IPAAm copolymers and copolymer-grafted surfaces

IPAAm co-polymers with each functional carboxylate monomer were synthesized as previously reported [16]. Briefly, purified IPAAm, co-monomer, and 2,2′-azobisisobutyronitrile (AIBN) as a free-radical initiator were dissolved in freshly distilled *N*,*N*-dimethylformamide (DMF). The ampoules containing the solution were de-gassed and then sealed by conventional methods, and immersed in a water bath held at 70 °C for 3 h. Copolymers were recovered by repeated precipitation into diethylether followed by drying as white powders. IPAAm copolymer-grafted dishes were prepared as previously reported [5,17]. Briefly, IPAAm monomer was dissolved in 2-propanol at a concentration of 55% (wt/wt). For preparation of IPAAm copolymer-grafted surfaces, either CIPAAm or CNPAAm monomer was added in ratios of 1, 3 and 5 mol% to total monomer concentration in 2-propanol. These monomer solutions were spread uniformly over tissue culture polystyrene dishes (TCPS) dishes (Falcon 3001, Becton Dickinson Labware, Oxnard, CA) and then electron-beam irradiated using an area beam electron processing system (Curetron EBC-200-AA2, Nissin High Voltage Co. Ltd., Kyoto, Japan) at a radiation dose of 0.3 MGy (acceleration voltage of 150 kV under 1.0×10^{-4} Pa). Monomers were polymerized and covalently grafted onto dish surfaces by this electron beam irradiation. Unreacted monomer and ungrafted polymer were then removed by washing extensively with cold water. The amount of grafted polymer was determined by attenuated total reflection Fourier transform infrared spectrophotometry (ATR-FTIR) as previously described [17]. Since the base substrate comprises TCPS, absorption at 1600 cm^{-1} results from the TCPS mono-substituted aromatic ring. As PIPAAm and its copolymers are grafted onto the TCPS surface, strong amide absorption appears in the region of 1650 cm^{-1}. The peak intensity ratio (I_{1650}/I_{1600}) was used to determine grafted density on the surface using the calibration curve of a known PIPAAm amount cast onto TCPS from solution.

2.3. Apparent pK′a measurements for new monomers and respective copolymers

Apparent dissociation constants (K'a) of the carboxylate-containing copolymers were determined from titration using the Henderson-Hasselbalch equation [18]. Each copolymer (100 mg) was dissolved in 10 ml of water, and 2 ml of 0.1 N HCl was added (final pH = 10) so that all carboxyl groups remained in the acid form. Typical carboxylate pK'a for AAc is 4.26. Then, ionized carboxyl groups and added HCl were titrated with 0.05 N NaOH(aq) under nitrogen. The pH where half the carboxyl groups in each copolymer were dissociated stoichiometrically was defined as the apparent pK'a.

2.4. Fluorescence measurements to determine phase transitions

Aqueous phase transition changes for all copolymers across their LCST values were determined by fluorescent measurements [19,20]. Pyrene was used as a hydrophobic fluorescent probe [21]. Fluorescent spectra were recorded on a spectrofluorometer (FP-770, Japan Spectroscopic Co., Tokyo, Japan). The temperature in a water-jacketed cell was controlled with a thermostated circulating bath to ±0.1 °C. Pyrene dissolved in acetone (2.0×10^{-4} M, 10 μl) was added to 4 ml of aqueous polymer solutions (2.5 mg/ml) in Dulbecco's phosphate buffered saline (PBS, pH 7.4). These samples

containing pyrene (5×10^{-7} M) were kept for 24 h at 20 °C before any measurements to allow complete evaporation of acetone. Fluorescence spectra of pyrene solutions contain a vibrational band exhibiting high sensitivity to the polarity of the pyrene environment [22]. From pyrene emission spectra, the intensity (peak height) ratios (I_1/I_3) of the first band (I_1: 374 nm) to the third band (I_3: 385 nm) were plotted as a function of temperature.

2.5. Water contact angle measurements as a function of time and temperature

IPAAm copolymer-grafted TCPS dishes were cut in size to 1.0×3.0 cm. Water contact angle was determined by the sessile drop method with a FACE contact angle meter (image processing type CA-X, Kyowa Interface Science, Saitama, Japan) using Dulbecco's modified Eagle's medium (DMEM, Iwaki, Chiba, Japan). The temperature was controlled by circulating water from a thermostated water bath (±0.1 °C). All samples were measured five times and averaged. Temperature was continuously recorded in situ.

2.6. Cell attachment/detachment assay

Bovine aortic endothelial cells (BAECs) were provided by Health Science Research Resources Bank (JCRB 0099; Osaka, Japan). BAECs were maintained on TCPS dishes with DMEM supplemented with 10% fetal bovine serum (FBS), 100 units/ml penicillin, and 100 μg/ml streptomycin at 37 °C in humidified atmosphere with 5% CO_2. After expansion, BAECs were harvested from TCPS dishes by treatment with 0.25% trypsin-0.26 mM EDTA in PBS. These cells were then plated onto the copolymer-grafted TCPS dishes at a density of 1.0×10^4 cells/cm^2 and cultured at 37 °C. Cell morphology was observed at certain time points and microphotographed under a phase contrast microscope. Spread cell numbers were counted on printed photographs. The ratio of spread cell density on copolymer-grafted surface to that on PIPAAm-grafted surface were presented as relative spread cell density. For low temperature treatments, spread cells were transferred to a CO_2 incubator equipped with a cooling unit fixed at 20 °C. The percentages of detached cell numbers after 30-min incubation at 20 °C to the total cell numbers visible were presented as detached cell ratios. All experiments were performed in triplicate and averaged. Statistics were calculated using SigmaStat 10.0 (SPSS, Chicago, IL).

3. Results and discussion

3.1. Copolymer phase transition behaviors

Temperature-responsive changes of P(IPAAm-*co*-CIPAAm) (CIPAAm 4.8 mol%) and P(IPAAm-*co*-CNPAAm) (CNPAAm 4.0 mol%) were examined using pyrene as a hydrophobic probe [21]. Fig. 2 shows the fluorescence intensity ratios (I_1/I_3) reflecting microenvironmental hydrophobicity surrounding pyrene [22]. Low I_1/I_3 values resulted from polymer collapsed hydrophobic environments, that is, polymer chains are hydrophobic and aggregate to change probe partitioning and fluorescence. PIPAAm solutions showed

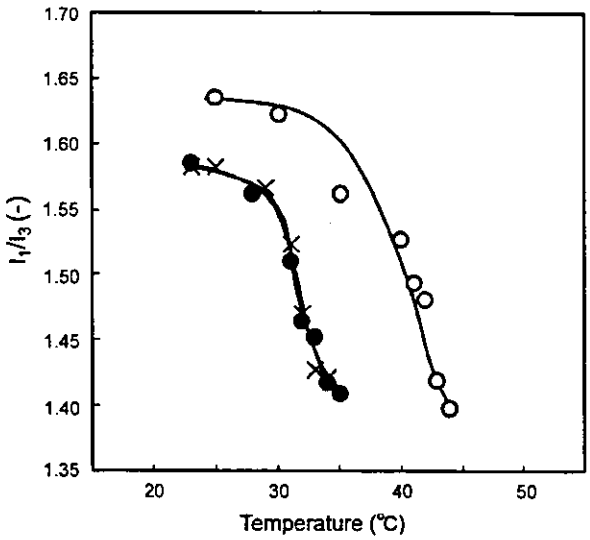

Fig. 2. Fluorescence measurements of IPAAm-based copolymer solutions at pH 7.4. The fluorescence intensity ratio I_1/I_3 reflects the microenvironmental hydrophobicity surrounding pyrene [22]. Pure PIPAAm: crosses, P(IPAAm-*co*-CIPAAm) (CIPAAm content 4.8 mol%): closed circles, P(IPAAm-*co*-CNPAAm) (CNPAAm content 4.0 mol%): open circles.